Solitary Waves and Fluctuations in Fragile Matter

Upadhyaya, N.

SUPPLEMENTARY MATERIAL

A

NESTERENKO SOLITARY WAVE

In this supplementary chapter, we review the original derivation of the strongly non-linear Nesterenko wave equation and motivate, how its solitary wave solution may be interpreted as a quasi-particle with an effective mass [32].

Consider a one dimensional chain of identical spherical particles of radius R with an initial overlap δ_0 (see Fig. (A.1)), and interacting with a non-linear force of the Hertz form. If the displacement of particle i from its equilibrium position is u_i, then the equation of motion of the i-th particle is

$$\ddot{u}_i = A(\delta_0 - u_i + u_{i-1})^{\frac{3}{2}} - A(\delta_0 - u_{i+1} + u_i)^{\frac{3}{2}}, \tag{A.1}$$

where $A = R^{\frac{1}{2}} 2^{\frac{-3}{2}} \Theta^{-1}$ and $\Theta = \frac{3(1-\nu^2)}{4E}$ is a material constant depending upon the Young's modulus E and Poisson's ratio ν. Here, double dots refer to two derivatives with respect to time t. If the displacement of the particles with respect to the initial pre-compression is small, i.e., $|u_{i-1} - u_i| \ll \delta_0$, the right hand side of Eq. (A.1) can be expressed as

$$\ddot{u}_i = A\delta^{\frac{3}{2}} \left[\left(1 + \frac{u_{i-1} - u_i}{\delta_0} \right)^{\frac{3}{2}} - \left(1 + \frac{u_i - u_{i+1}}{\delta_0} \right)^{\frac{3}{2}} \right]. \tag{A.2}$$

Using the binomial expansion, i.e., $(1+x)^{\frac{3}{2}} \approx 1 + \frac{3}{2}x + \frac{3}{4}x^2 \cdot \cdot$, the right hand side of Eq. (A.2) can be expressed as

$$\ddot{u}_i = c(u_{i+1} - 2u_i + u_{i-1}) + d(u_{i+1} - 2u_i + u_{i-1})(u_{i-1} - u_{i+1}) \tag{A.3}$$

where, $c = \frac{3}{2} A \delta_0^{\frac{3}{2}}, d = \frac{3}{8} A \delta_0^{\frac{-1}{2}}$. For a long wavelength continuum approximation $L \gg a = 2R$, where a is the lattice spacing, we now make the simplification $u_i \to u(x) \equiv u$, where x is the continuum spatial variable. Thus, we obtain

$$\begin{aligned} u_{tt} = c(u(x+a) - 2u(x) + u_(x-a)) + \\ d(u(x+a) - 2u(x) + u(x-a))(u(x-a) - u(x+a)). \end{aligned} \tag{A.4}$$

Taylor expanding the right hand side and retaining terms to order a^4, we obtain the weakly non-linear wave equation

$$u_{tt} = c_0^2 u_{xx} + 2c_0 \gamma u_{xxxx} - \epsilon u_x u_{xx}, \tag{A.5}$$

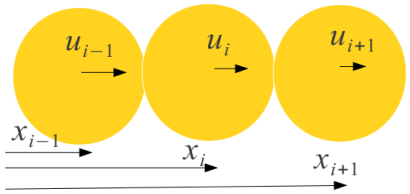

Figure A.1: Nearest neighbour particles in a one dimensional granular chain.

where, $c_0^2 = A\delta_0^{\frac{1}{2}}6R^2, \gamma = \frac{c_0}{6}R^2, \epsilon = c_0^2\frac{R}{\delta_0}$. Here, subscripts refer to partial derivatives with respect to space x and time t. This equation is known as the Boussinesq equation and under certain approximations, the solutions of this equation satisfy the better known Korteweg-De Vries (KdV) equation.

However, our main interest is in the other regime where $\delta_0 \to 0$ and thus the standard long wavelength approximation made above can no longer be used, since $|u_{i-1} - u_i| \gg \delta_0$. Consequently, we take the extreme limit and set $\delta_0 = 0$ (the spherical beads just touching other) in Eq. (A.1) and express it in the continuum space and time variables as

$$\ddot{u}_i = A\left[(u(x-a)-u(x))^{\frac{3}{2}} - (u(x)-u(x+a))^{\frac{3}{2}}\right], \qquad (A.6)$$

and Taylor expand as

$$\ddot{u}_i = A\left(u - au_x + a^2/2u_{xx} - \frac{a^3}{6}u_{xxx} + \frac{a^4}{24}u_{xxxx} - u\right)^{\frac{3}{2}} - \qquad (A.7)$$

$$A\left(u - u - au_x - \frac{a^2}{2}u_{xx} - \frac{a^3}{6}u_{xxx} - \frac{a^4}{24}u_{xxxx}\right)^{\frac{3}{2}}. \qquad (A.8)$$

Now performing a Binomial expansion around $(-u_x)$, we obtain the Nesterenko equation for strongly non-linear waves:

$$u_{tt} = c^2\left[\frac{3}{2}(-u_x)^{\frac{1}{2}}u_{xx} + \frac{a^2}{8}(-u_x)^{\frac{1}{2}}u_{xxxx} - \frac{a^2u_{xx}u_{xxx}}{8(-u_x)^{\frac{1}{2}}} - \frac{a^2(u_xx)^3}{64(-u_x)^{\frac{1}{2}}}\right] \qquad (A.9)$$

where,$c^2 = (2R)^{\frac{5}{2}}\frac{A}{m}$ is just a rescaled material dependent parameter. Upon rewriting this equation in terms of the strain field $\xi = -u_x$, we obtain the equation in a more condensed form

$$\xi_{tt} = c^2\left[\xi^{\frac{3}{2}} + \frac{2R^2}{5}\xi^{\frac{1}{4}}(\xi^{\frac{5}{4}})_{xx}\right]_{xx}. \qquad (A.10)$$

A travelling wave solution of Eq. (A.10) is obtained by looking for solutions of the form $\xi = \xi(x - v_s t)$, where v_s is the speed of propagation. Upon substituting in Eq. (A.10) and integrating twice [32], we obtain the solitary wave solution (see Supplementary Information B for a similar calculation in more detail)

$$\xi = \left(\frac{5}{4}\frac{v_s^2}{c^2}\right)^2 \cos^4\left(\frac{\sqrt{10}}{5a}(x - v_s t)\right). \tag{A.11}$$

This represents a propagating strain field ξ. Often in simulations, it is easier to measure the velocity field $v(x,t) = u(x,t)_t = -v_s \xi(x,t)$. Thus, the solution in terms of the velocity field reads

$$v = \left(\frac{25}{16}\frac{v_s^5}{c^4}\right) \cos^4\left(\frac{\sqrt{10}}{5a}(x - v_s t)\right). \tag{A.12}$$

where, we find that the amplitude of the wave depends upon the speed of propagation as $\xi_m \equiv u_p \sim v_s^5$. This is also the scaling relation we found for compressional shocks in amorphous packings in subsection 1.1.4.1. Notice, the width of the solitary wave is simple a few times the grain diamter a , w=$\frac{5a}{\sqrt{10}}$ and is independent of the speed of propagation v_s. This is unlike some well known weakly non-linear waves such the KdV equation, where the width also depends upon the speed of propagation.

A.1 QUASI-PARTICLE INTERPRETATION

The solitary wave kinetic energy K_{SW}, the potential energy U_{SW}, the total energy E_{SW} and momentum P_{SW} (i.e, sum of the respective kinetic, potential and total energies of the beads that are enveloped by the solitary wave) are-

$$K_{SW} = \frac{m v_s^2}{4R}\int dx \xi^2 = \left[\frac{(2R)^3 \xi_m^{\frac{5}{2}}}{\Theta\sqrt{10}} W_8\right] \tag{A.13}$$

$$U_{SW} = \frac{2A(2R)^{\frac{3}{2}}}{5}\int dx \xi^{\frac{5}{2}} = \left[\frac{(2R)^3 \xi_m^{\frac{5}{2}}}{\Theta\sqrt{10}} W_{10}\right] \tag{A.14}$$

$$E_{SW} = \left[\frac{(2R)^3 \xi_m^{\frac{5}{2}}}{\Theta\sqrt{10}} (W_8 + W_{10})\right] \tag{A.15}$$

$$P_{SW} = \frac{m v_s}{2R}\int dx \xi = \left[\frac{(2R)^3 \xi_m^{\frac{5}{4}}}{\sqrt{\frac{3\Theta}{\pi\rho}}} W_4\right]. \tag{A.16}$$

where, $W_n = \int_0^{\frac{\pi}{2}} dx \cos^n x$ [17].

Now, the proportionality of the solitary wave kinetic energy K_{SW} and potential energy U_{SW}, gives the opportunity to describe its dynamics as a quasi-particle. Defining an equivalent particle of mass m_{SW} moving at a speed v_{SW} such that the solitary wave momentum and energy are $P_{SW} = m_{SW} V_{SW}$ and $E_{SW} = \frac{1}{2} m_{SW} V_{SW}^2$, one finds

$$m_{SW} = \frac{P_{SW}^2}{2E_{SW}} = \Omega x m, \tag{A.17}$$

where, $\Omega = \frac{W_4^2 \sqrt{10}}{W_8 + W_{10}} = 1.345$. Thus, the solitary wave is effectively like a particle with a rescaled mass $1.34m$, where m is the mass of the beads. Note, for many waves, differentiating E_{SW} with respect to P_{SW} gives the group velocity or the speed of propagation of the wave. However, here P_{SW} is not the canonical momentum and is physically related to the speed of the particles, not the wave.

An important relation to be used later, is between the solitary wave momentum P_{SW}, the mass of the beads m and the solitary wave speed of propagation v_s. Using $P_{SW} \equiv m \int dx \frac{du}{dt} \sim m v_s \int dx \xi$ and substituting the solitary wave solution for ξ, we find the relation

$$\begin{aligned} P_{SW} &= m v_s \xi_m \int dx \cos^4 x, && \text{(A.18)} \\ &= m v_s^5 \left(\frac{5}{6} \pi \rho \Theta\right)^2 \int dx \cos^4 x, && \text{(A.19)} \\ &\sim m^3 v_s^5, && \text{(A.20)} \end{aligned}$$

where $\rho = \frac{m}{(4/3\pi R^3)}$. In Supplementary information B, we provide an alternative (albeit approximate) derivation of the strongly nonlinear Nesterenko wave equation that would allow us to express the solitary wave solution for any general nonlinear exponent $\alpha > 2$.

B

SOLITARY WAVE SOLUTION

In this supplementary chapter, we will derive the quasi-particle representation of the solitary wave using an approximation to the Nesterenko solitary wave equation, that is valid for a more general non-linear interaction potential with exponent $\alpha > 2$ [49].

B.1 ROSENAU APPROXIMATION

Here, we adopt as our starting point the Lagrangian for a one dimensional chain of identical spheres that are just touching each other, i.e., in the limit $\delta_0 \to 0$ (strongly nonlinear limit) -

$$L = \sum_n \frac{1}{2} m \dot{u}_n^2 - \frac{A}{\alpha} \left(\frac{u_n - u_{n+1}}{a} \right)^\alpha \tag{B.1}$$

where, u_n is the displacement of the $n-$th sphere from its equilibrium position and $a = 2R$ is the lattice spacing. In order to avoid doing a Binomial expansion in powers of α, we will define the continuum field variable as

$$a\phi'(n + \frac{1}{2}) = u_{n+1} - u_n, \tag{B.2}$$

where, primes denote derivative with respect to x. We now take the continuum limit, i.e., $u_n \to u(x) \equiv u$ and Taylor expand the right hand side about $x + \frac{a}{2}$:

$$a\phi'(x) \approx u + \frac{a}{2}u' + \frac{a^2}{8}u'' + \frac{a^3}{48}u''' - u + \frac{a}{2}u' - \frac{a^2}{8}u'' + \frac{a^3}{48}u'''. \tag{B.3}$$

Integrating both sides once with respect to x, we obtain

$$\phi(x) = u + \frac{a^2}{24}u'', \tag{B.4}$$

$$= \left(1 + \frac{a^2}{24}\frac{d^2}{dx^2}\right) u(x). \tag{B.5}$$

Inverting the differential operator, we obtain

$$u(x) \approx \phi - \frac{a^2}{24}\phi''. \tag{B.6}$$

Thus, in the contiuum limit, the Lagrangian becomes

$$\frac{L}{m} = \int dx \frac{1}{2}\dot{u}^2(x) - \frac{A}{m\alpha}\left(\phi'(x)\right)^{\alpha} \tag{B.7}$$

$$= \int dx \frac{1}{2}\dot{\phi}^2 - \frac{a^2}{24}\dot{\phi}\dot{\phi}'' - \frac{A}{m\alpha}\left(\phi'\right)^{\alpha}. \tag{B.8}$$

By using the Euler-Lagrange equation, we obtain the equation of motion as

$$\ddot{\phi} - \frac{a^2}{12}\ddot{\phi}'' + \frac{A}{m}\left[(-\phi')^{\alpha-1}\right]' = 0. \tag{B.9}$$

Note, ϕ here corresponds to the continuum displacement field. The corresponding equation in the strain field $\delta = -\phi'$ reads

$$\ddot{\delta} - \frac{a^2}{12}\ddot{\phi}'' - \frac{A}{m}\left[\delta^{\alpha-1}\right]'' = 0. \tag{B.10}$$

B.2 SOLITARY WAVE SOLUTION

The solitary wave solution of Eq. (B.10) can be obtained by looking for propagating solutions of the form $\delta(x,t) = \delta(x - v_s t)$:

$$\frac{v_s^2 a^2}{12}\delta'' - v_s^2\delta + \frac{k}{m}\delta^{\alpha-1} = 0, \tag{B.11}$$

which can be expressed in the form of Newtons's-like equation

$$\delta'' = -\frac{12}{v_s^2 a^2}\left[-v_s^2\delta + \frac{k}{m}\delta^{\alpha-1}\right] = -\frac{dW}{d\delta}. \tag{B.12}$$

Multiplying both sides by δ' and integrating,

$$\int dx\delta'\delta'' = \int dx - \frac{dW}{d\delta}\delta', \tag{B.13}$$

$$\int \frac{1}{2}d(\delta')^2 = \int -dW, \tag{B.14}$$

$$\frac{1}{2}(\delta')^2 = -W(\delta). \tag{B.15}$$

Integrating again, we find

$$\int \frac{d\delta}{\sqrt{-2W}} = \int dx. \tag{B.16}$$

Substituting, $W(\delta) = \frac{12}{v_s^2 a^2}\left[\frac{k}{m\alpha}\delta^{\alpha} - \frac{v_s^2}{2}\delta^2\right]$, and writing for brevity $A = \frac{12}{v_s^2 a^2}\frac{k}{m\alpha}$ and $B = \frac{6}{a^2}$, we need to integrate

$$\int \frac{d\delta}{\sqrt{2B\delta^2 - 2A\delta^{\alpha}}} = x, \tag{B.17}$$

$$\int \frac{d\delta}{\sqrt{2}\delta\sqrt{B - A\delta^{\alpha-2}}} = x. \tag{B.18}$$

Making the change of variables, $z^2 = B - A\delta^{\alpha-2}$, we find

$$\frac{-\sqrt{2}}{A(\alpha-2)} \int \frac{dz}{\delta^{\alpha-2}} = x, \tag{B.19}$$

$$\frac{-\sqrt{2}}{(\alpha-2)} \int \frac{dz}{(\sqrt{B})^2 - z^2} = x. \tag{B.20}$$

Therefore,

$$x = \frac{-1}{\sqrt{2B}(\alpha-2)} \left[\int \frac{dz}{\sqrt{B}-z} + \int \frac{dz}{\sqrt{B}+z} \right], \tag{B.21}$$

yielding

$$s = -\sqrt{2B}(\alpha-2)x = \ln \frac{\sqrt{B}+z}{\sqrt{B}-z}, \tag{B.22}$$

or

$$z = -\sqrt{B}\frac{1-\exp -s}{1+\exp -s}. \tag{B.23}$$

Squaring and substituting $z^2 = B - A\delta^{\alpha-2}$,

$$B - A\delta^{\alpha-2} = B\frac{\exp s/2 - \exp -s/2}{\exp s/2 + \exp -s/2}, \tag{B.24}$$

yielding,

$$\delta^{\alpha-2} = \frac{B}{A}\operatorname{sech}^2(s/2). \tag{B.25}$$

Therefore, the solitary wave solution is

$$\delta = \left(\frac{m\alpha V_s^2}{2K}\right)^{\frac{1}{\alpha-2}} \operatorname{sech}^{\frac{2}{\alpha-2}} \left(\frac{\sqrt{3}}{2a}(x - V_s t)\right). \tag{B.26}$$

We now note a few important properties of the solitary wave solution.

- The width of the solitary wave is approximately $w = \frac{2}{\sqrt{3}}$ times the lattice spacing $a = 2R$. Thus, unlike the Nesterenko solitary wave that is explicitly 5 particle diameters wide, the approximate width predicted by the solitary wave solution above is much less.
- However, due to the secant-hyperbolic function, Eq. (B.26) has an exponential tail. In principle this means, that unlike the Nesterenko solitary wave Eq. (A.12) that is zero outside 5 particle diameters (due to the zeros of cosine function), the above solution is never strictly zero. Thus, Eq. (B.26) is said to lack a compact support.

- The Hamiltonian and therefore the conserved energy corresponding to the Lagrangian Eq. (B.8) is

$$\frac{H}{m} = \int dx \frac{1}{2}\dot{\phi}^2 - \frac{a^2}{24}\dot{\phi}\dot{\phi}'' + \frac{A}{m\alpha}\left(\phi'\right)^{\alpha}. \tag{B.27}$$

  Similarly, the momentum of the beads (not the canonical momentum) is simply,

$$\frac{P}{m} = \int dx \dot{\phi}. \tag{B.28}$$

  In conjunction, these two relations again allow us to interpret the solitary wave as a quasi-particle.

C

HYDRODYNAMICAL MODES AND POWER SPECTRUM

C.1 HYDRODYNAMIC MODES

In this supplimenrary section, we derive the longitudinal and transverse power spectral densities, that is used to obtain an understanding of the emergent state in Chapter 4 [72].

We begin with the fluid equations of continuity and the Navier-Stokes equation for the conservation of momentum [69] (ignoring any fluctuations in temperature of the system),

$$\frac{\partial}{\partial t}\tilde{\rho}(\mathbf{r},t)+\nabla\cdot[\tilde{\rho}(\mathbf{r},t)\tilde{\mathbf{v}}(\mathbf{r},t)]=0, \tag{C.1}$$

where $\tilde{\rho}(\mathbf{r},t)\equiv n_d(\mathbf{r},t)$ is the particle number density per unit area and

$$m\frac{\partial}{\partial t}[\tilde{\rho}(\mathbf{r},t)\tilde{\mathbf{v}}(\mathbf{r},t)]+m\tilde{\rho}(\mathbf{r},t)[\tilde{\mathbf{v}}(\mathbf{r},\mathbf{t})\cdot\nabla]\tilde{\mathbf{v}}(\mathbf{r},\mathbf{t})=-\nabla\tilde{p}(\mathbf{r},t)+\eta_1\{\nabla^2\tilde{\mathbf{v}}(\mathbf{r},t)+\nabla[\nabla\cdot\tilde{\mathbf{v}}(\mathbf{r},\mathbf{t})]\} \tag{C.2}$$

where, m is the mass of a particle, $\tilde{p}(\mathbf{r},t)$ is the pressure, $\tilde{\mathbf{v}}(\mathbf{r},t)\equiv\mathbf{v_d}(\mathbf{r},\mathbf{t})$ is local velocity field, and η_1 is the coefficient of shear viscosity [69]. Here, the expressions have been written for a fluid assumed to be in a two dimensional plane. Further, we have ignored any contributions coming from a bulk viscosity [69, 72].

We focus on studying small deviations from local equilibrium. Note, in the process of studying small deviations from equilibrium, we are implicitly studying small amplitude variations in a compressible fluid , which by definition is a *sound wave* if we consider longitudinal fluctuations.

Next, we choose a reference frame that moves with the fluid velocity, say $\tilde{\mathbf{v}}_\mathbf{0}$ that we will take to be zero for a fluid at rest. We then linearize the above equations by considering small perturbations to first order, as follows

$$\tilde{\rho}=\tilde{\rho}_0+\epsilon\tilde{\rho}_1=\rho+\delta\rho, \tag{C.3a}$$

$$\tilde{p}=\tilde{p}_0+\epsilon\tilde{p}_1=p+\delta p, \tag{C.3b}$$

$$\tilde{\mathbf{v}} = \tilde{\mathbf{v}}_0 + \epsilon\tilde{\mathbf{v}}_1 = 0 + \mathbf{v}. \tag{C.3c}$$

Defining the current density as $\mathbf{j}(\mathbf{r}, t) = \rho\mathbf{v}(\mathbf{r}, t)$ and linearizing Eq. (C.1) and Eq. (C.2) with respect to small perturbations, one obtains to first order

$$\frac{\partial}{\partial t}\delta\rho(\mathbf{r}, t) + \nabla \cdot \mathbf{j}(\mathbf{r}, t) = 0, \tag{C.4a}$$

$$m\frac{\partial}{\partial t}\mathbf{j}(\mathbf{r}, t) + \nabla\delta p(\mathbf{r}, t) = \frac{\eta_1}{\rho}\{\nabla^2\mathbf{j}(\mathbf{r}, t) + \nabla[\nabla \cdot \mathbf{j}(\mathbf{r}, t)]\} \tag{C.4b}$$

Dividing the momentum conservation equation by m, and defining $\frac{\eta_1}{m\rho} = \nu_1$,

$$\frac{\partial}{\partial t}\mathbf{j}(\mathbf{r}, t) + \frac{\nabla\delta p(\mathbf{r}, t)}{m} = \nu_1\{\nabla^2\mathbf{j}(\mathbf{r}, t) + \nabla[\nabla \cdot \mathbf{j}(\mathbf{r}, t)]\} \tag{C.5}$$

We now take the Fourier transform of Eqs. (C.4a) and Eq. (C.5) in position space, i.e., transform $\mathbf{j}(\mathbf{r}, t) \to \mathbf{j}_\mathbf{k}(t)$, $\delta p(\mathbf{r}, t) \to \delta p_\mathbf{k}(t)$ and $\delta\rho(\mathbf{r}, t) \to \delta\rho_\mathbf{k}(t)$ with $\mathbf{k} = (k, 0)$ being the k-space vector, that we will take to be in the x-direction. Further, let us define components of the current density vector as $\mathbf{j}_\mathbf{k}(t) = (j^l_k(t), j^t_k(t))$, where $j^l_k(t)$ is the longitudinal part of the current density, pointing in the direction of k-vector (x direction in this case) and $j^t_k(t)$ is the transverse component, pointing in a direction perpendicular to k-vector (y-direction in this case). We thus obtain the following equations in Fourier space

$$\frac{\partial}{\partial t}\delta\rho_k(t) - ikj^l_k(t) = 0, \tag{C.6a}$$

$$\frac{\partial}{\partial t}j^l_k(t) - \frac{ik\delta p_k(t)}{m} = \nu_1[-k^2j^l_k(t) - k^2j^l_k(t)] - \nu_2k^2j^l_k(t), \tag{C.6b}$$

$$\frac{\partial}{\partial t}j^t_k(t) = -\nu_1k^2j^t_k(t). \tag{C.6c}$$

Note, by taking the Fourier transform, we have managed to decouple the longitudinal fluctuations in Eq. (C.6b) and transverse fluctuations, Eq. (C.6c). However, the longitudinal fluctuations are coupled to density fluctuations, Eq. (C.6a), that eventually gives rise to a finite sound speed in the longitudinal direction. Conversely, as seen in Eq. (C.6c), transverse waves are purely diffusive and de-coupled from any density fluctuations.

C.1.1 *Longitudinal Current Density*

We now focus on the longitudinal current density, Eqs . (C.6a) and (C.6b) and drop the superscripts and subscripts l. An analogous calculation can be done for the transverse current density.

First, Eq. (C.6a) may be written in its integral form as

$$\delta\rho_k(t) = \delta\rho_k(0) + ik\int_0^t dt'\, j_k(t'). \tag{C.7}$$

Recall, in the Navier-Stokes equation, we ignored any temperature fluctuations. Thus, as a working assumption, we are considering an ensemble with constant temperature and a fixed number of particles N. Thus, we write the variations in pressure as

$$\delta p = \left[\frac{\delta p}{\delta\rho}\right]_{N,T}\delta\rho \tag{C.8}$$

From thermodynamics [70], we identify this as

$$\left[\frac{\delta p}{\delta\rho}\right]_{N,T} = \frac{1}{\rho\chi_T}, \tag{C.9}$$

where χ_T is the isothermal compressibility of the system. Defining, $2\nu_l = \nu_l$, where ν_l is the longitudinal viscosity, we write Eq. (C.6b) as

$$\frac{\partial}{\partial t}j_k(t) - \frac{ik\delta\rho_k(t)}{m\rho\chi_T} = -\nu_l k^2 j_k(t). \tag{C.10}$$

Inserting Eq. (C.7) into the above equation, we obtain

$$\frac{\partial}{\partial t}j_k(t) = -\frac{k^2}{m\rho\chi_T}\int_0^t dt'\, j_k(t') - \nu_l k^2 j_k(t) + \frac{ik}{m\rho\chi_T}\delta\rho_k(0) \tag{C.11}$$

The longitudinal current density auto-correlation function is defined as [69]

$$C(k,t) = \langle j_k^*(0) j_k(t)\rangle. \tag{C.12}$$

Multiplying Eq. (C.11) by $j_k(0)^*$ and ensemble averaging,

$$\frac{\partial}{\partial t}C(k,t) = -\frac{k^2}{m\rho\chi_T}\int_0^t dt'\, C(k,t') - \nu_l k^2 C(k,t), \tag{C.13}$$

where $\frac{ik}{m\rho\chi_T}\langle\rho_k(0)j_k^*(0)\rangle$ vanishes by symmetry [69], as can be seen by multiplying Eq. (C.6a) with $\rho_k(0)^*$ and ensemble averaging the resultant expression, evaluated at $t = 0$. Further, it

can be shown that $\langle \frac{\partial \rho_k(t)}{\partial t} \rho_k^*(0) \rangle_{t=0}$ vanishes [69], producing the desired result.

The power spectrum of the longitudinal current density auto-correlation function can now be obtained as the Fourier transform of the longitudinal current density auto-correlation function or equivalently, as the real part of the one sided Laplace transform [70] of the current density auto-correlation function, evaluated at $s = i\omega$, which we call $P(k,\omega) = \Re\{\mathcal{L}[C(k,t)]\}_{s=i\omega}$. Thus, taking the Laplace transform of Eq. (C.13), we obtain

$$sP(k,s) - P(k,0) = -\frac{k^2}{m\rho\chi_T}\frac{P(k,s)}{s} - \nu_l k^2 P(k,s), \tag{C.14}$$

and therefore,

$$P(k,s) = P(k,0)\frac{s}{s^2 + \omega_0^2 + s\nu_l k^2}, \tag{C.15}$$

where, we have defined $\omega_0^2 = \frac{k^2}{m\rho\chi_T}$. Taking twice the real part, evaluated for $s = i\omega$, we finally obtain

$$P(k,s) = 2P(k,0)\frac{\omega^2 \nu_l k^2}{\left[\omega^2 - \omega_0^2\right]^2 + (\omega\nu_l k^2)^2}, \tag{C.16}$$

that is Eq. (4.7) in the main text. Note, for fluids, the constant $P(k,0) = v_{th}^2$ is basically square of the average thermal speed of particles [69].

D

FLUCTUATION DISSIPATION THEOREM

In this section, we will review the derivation for the appropriate form of the noise term that along with a second order hydrodynamical damping term satisfies the fluctuation dissipation theorem [64]. Consider the discrete set of equations

$$\begin{aligned} \frac{dp_n}{dt} &= t_n + f_n^{\text{Noise}} + f_n^{\text{Damping}}, \\ \frac{dx_n}{dt} &= \frac{p_n}{M}, \end{aligned} \tag{D.1}$$

where,

$$t_n = -\frac{\partial H}{\partial x_n} = -\frac{\partial U}{\partial x_n}, \tag{D.2}$$

$$f_n^{\text{Damping}} = m\nu\left(\frac{dx_{n+1}}{dt} - 2\frac{dx_n}{dt} + \frac{dx_{n-1}}{dt}\right), \tag{D.3}$$

and we need to determine the form of f_n^{Noise} that satisfies the fluctuation dissipation theorem. Here, p_n denotes the momentum, x_n the longitudinal displacement from its equilibrium position of the $n-$th particle with mass m and velocity dx_n/dt. The Hamiltonian is $H = K + U$, where $K = \sum_n \frac{p_n^2}{2m}$ is the kinetic energy and $U = \sum_n V[x_{n+1} - x_n]$ is the potential energy for a general inter-particle potential V that depends upon the relative displacement between neighbouring masses.

Taking the discrete (spatial) Fourier transform of Eqs. (D.1), i.e., $x_n = \frac{1}{\sqrt{N}}\sum_k \exp(-ikn)X_k$ and $p_n = \frac{1}{\sqrt{N}}\sum_k \exp(-ikn)P_k$ we obtain

$$\begin{aligned} \frac{dP_k}{dt} &= T_k + F_k^{\text{Noise}} + \nu\left[\exp(-ik) + \exp(ik) - 2\right]\frac{dX_k}{dt}, \\ \frac{dP_k}{dt} &= T_k + F_k^{\text{Noise}} - \nu\gamma_k P_k, \\ \frac{dX_k}{dt} &= \frac{P_k}{M}. \end{aligned} \tag{D.4}$$

where, from the damping term we have defined

$$\gamma_k = 2\left[1 - \cos(k)\right]. \tag{D.5}$$

We define

$$F_k^{\text{Noise}}(t) = \sqrt{D(k)}\xi_k(t), \tag{D.6}$$

where, $\xi_k(t)$ is a delta correlated white noise,

$$\langle \xi_k(t)\xi_{k'}(t')\rangle = \delta(t-t't)\delta_{k,-k'} \tag{D.7}$$

and $D(k)$ is to be determined.

The associated multi-dimensional Fokker-Planck equation [67] of Eqs. (D.4) takes the form

$$\partial_t \rho = \sum_k \left[-\partial_{P_k}(T_k\rho_k) - \frac{P_{-k}}{M}\partial_{X_{-k}}\rho_k + \nu\gamma_k\partial_{P_k}\left(P_k\rho_k + \frac{D(k)}{2\nu\gamma_k}\partial_{P_{-k}}\rho_k\right)\right] \tag{D.8}$$

where,$\rho = \langle \prod_k \delta\left[P_k - P_k(t)\right]\delta\left[X_k - X_k(t)\right]\rangle$.

In order to determine $D(k)$, we assume the stationary solution of Eq. (D.8) to be the Boltzmann distribution, i.e.,

$$\rho = N\exp\left(-\frac{H}{k_B T}\right), \tag{D.9}$$

where H is the Hamiltonian and N is a normalization constant. Substituting Eq. (D.9) into Eq. (D.8), we find that for a stationary distribution the left hand side must be zero. Consider, the first term on the right hand side

$$\begin{aligned} -\partial_{P_k}(T_k\rho_k) &= -\rho_k\partial_{P_k}T_k - T_k\partial_{P_k}\rho_k & \text{(D.10)}\\ &= 0 - T_k\frac{\partial\rho_k}{\partial H}\frac{\partial H}{\partial P_k} & \text{(D.11)}\\ &= \frac{T_k P_{-k}\rho}{M k_B T}, & \text{(D.12)} \end{aligned}$$

where we have used $\frac{\partial H}{\partial P_k} = \frac{P_{-k}}{2M}$ since in Fourier space, the kinetic part of the Hamiltonian assumes the form $K = \sum_k \frac{P_k P_{-k}}{2M}$. Similarly, the second term on the right evaluates to

$$\begin{aligned} -\frac{P_{-k}}{M}\partial_{X_{-k}}\rho_k &= -\frac{P_{-k}}{M}\frac{\partial\rho_k}{\partial H}\frac{\partial H}{\partial X_{-k}} & \text{(D.13)}\\ &= -\frac{T_k P_{-k}\rho}{M k_B T}, & \text{(D.14)} \end{aligned}$$

where we have used the relation $T_k = -\frac{\partial H}{\partial X_{-k}}$ (as can be checked for instance if the inter-particle potential is harmonic). Thus, the first two terms on the the right cancel out. Equating the third on the right of Eq. (D.8) to zero, we obtain

$$\begin{aligned} P_k\rho_k + \frac{D(k)}{2\nu\gamma_k}\frac{\partial\rho_k}{\partial H}\frac{\partial H}{\partial P_{-k}} &= 0, & \text{(D.15)}\\ P_k\rho_k - \frac{D(k)}{2\nu\gamma_k}\frac{\rho_k}{k_B T}\frac{P_k}{M} &= 0, & \text{(D.16)} \end{aligned}$$

and therefore,

$$D(k) = 2\nu\gamma_k M k_B T. \tag{D.17}$$

Now, from Eqs. D.6 and D.17, the noise term in position space is

$$f_n^{noise}(t) = 2\sqrt{2\nu M k_B T}\frac{1}{\sqrt{N}}\sum_k \exp(-ikn)\sin\left(\frac{k}{2}\right)\xi_k(t) \tag{D.18}$$

Therefore,

$$\frac{N\langle f_n^{noise}(t) f_{n'}^{noise}(t')\rangle}{8\nu M k_B T} = \sum_k\sum_{k'}\exp(-i[kn+k'n'])\sin\left(\frac{k}{2}\right)\sin\left(\frac{k'}{2}\right)\langle\xi_k(t)\xi_{k'}(t')\rangle.$$

Substituting the relation from Eq. (D.7) in the above equation, we obtain

$$\frac{N\langle f_n^{noise}(t) f_{n'}^{noise}(t')\rangle}{4\nu M k_B T} = -\delta(t-t')\sum_k \exp[-ik(n-n')](1-\cos(k)).$$

Taking the Fourier transform of the above equation, noting that

$$\begin{aligned}\frac{1}{N}\sum_k \exp[-ik(n-n')] &= \delta_{n,n'}\\ \frac{1}{N}\sum_k \exp[-ik(n-n')]\cos(k) &= \frac{1}{2}\left(\delta_{n,n'+1}+\delta_{n,n'-1}\right),\end{aligned}$$

we find,

$$\langle f_n^{noise}(t) f_{n'}^{noise}(t')\rangle = -2\nu M k_B T\delta(t-t')\left(\delta_{n+1,n'}-2\delta_{n,n'}+\delta_{n-1,n'}\right).$$

This relation can be satisfied by defining

$$f_n^{noise}(t) = \sqrt{2\nu M k_B T}\,[\xi_{n+1}(t)-\xi_n(t)] \tag{D.19}$$

with

$$\langle\xi_n(t)\xi_{n'}(t')\rangle = \delta(t-t')\delta_{n,n'}. \tag{D.20}$$

This is the fluctuation dissipation theorem we use in Eq. (5.3) in the main text.

E

LINEAR NON-QUASISTATIC REGIME

In the following supplementary section, we will solve for the analytic form of the transverse velocity field when the response of the random spring network falls in the linear frequency dependent regime. The derivation therefore rests on knowing the frequecy dependent elastic moduli. In addition, we will see how the same solution can be arrived at by starting with a fractional diffusion equation in real space and time. Here, the fractional exponent can be read off from the super-diffusive exponent that characterizes the broadening of the shear front width at early times.

E.1 FROM OSCILLATORY RHEOLOGY

Consider the general frequency dependent constitutive relation for a linear visco-elastic material:

$$\sigma(s) = G(s)\gamma(s)\,, \tag{E.1}$$

where, $G(s)_{s=i\omega} = G'(\omega) + iG''(\omega)$ is the (Laplace transformed) complex modulus, whose real and imaginary parts correspond to the storage and loss modulus respectively. The field $\sigma(s) \equiv \sigma_{xy}(s)$ denotes the shear stress and $\gamma(s) \equiv \gamma_{xy}(s)$ the shear strain. The general frequency dependent constitutive stress-strain relation Eq. (E.1) corresponds to the following convolution integral in the time domain,

$$\sigma(x,t) = \int_0^t G(\tau)\gamma(x,t-\tau)d\tau. \tag{E.2}$$

Substituting into the equation of motion

$$\frac{\partial\sigma(x,t)}{\partial x} = \rho\frac{\partial^2 u(x,t)}{\partial t^2} \tag{E.3}$$

and defining $v(x,t) = \frac{\partial u(x,t)}{\partial t}$, we obtain (interchanging the order of integration and differentiation),

$$\int_0^t G(\tau)\frac{\partial\gamma(x,t-\tau)}{\partial x}d\tau = \rho\frac{\partial v(x,t)}{\partial t}. \tag{E.4}$$

Differentiating once with respect to time t, we find

$$\left[G(\tau)\frac{\partial\gamma(x,t-\tau)}{\partial x}\right]_{\tau=t} + \int_0^t G(\tau)\frac{\partial^2\gamma(x,t-\tau)}{\partial x\partial t}d\tau = \rho\frac{\partial^2 v(x,t)}{\partial t^2}. \tag{E.5}$$

Since $\gamma(x,t) = \frac{\partial u(x,t)}{\partial x}$, the first term in the square brackets can be expressed as $G(t)\frac{\partial^2 u(x,0)}{\partial x^2}$, which evaluates to 0, since there is no displacement field at $t = 0$. Therefore,

$$\frac{\partial^2}{\partial x^2}\int_0^t G(\tau)v(x,t-\tau)d\tau = \rho\frac{\partial^2 v(x,t)}{\partial t^2}. \tag{E.6}$$

Transforming back to Laplace time (noting that the first term is just the convolution integral), we obtain

$$G(s)\frac{\partial^2 v(x,s)}{\partial x^2} = \rho s^2 v(x,s) - \rho s\left[v(x,t)\right]_{t=0} - \rho\left[\frac{\partial v(x,t)}{\partial t}\right]_{t=0} \tag{E.7}$$

Since we are solving in the domain $x > 0$, our initial condition is $v(x > 0, 0) = 0$ and boundary condition is $v(x = 0, t) = v_0$. Thus, the two terms on the right are 0 leaving us with

$$\frac{\partial^2 v(x,s)}{\partial x^2} = \frac{\rho s^2}{G(s)}v(x,s). \tag{E.8}$$

This is an ordinary differential equation in x, solving which we obtain:

$$v(x,s) = \frac{v_0}{s}\exp\left(x\frac{s}{\sqrt{G(s)}}\right). \tag{E.9}$$

In oscillatory rheology, it is found that in the frequency dependent regime, the elastic moduli scale as $G(s) \sim s^{\frac{1}{2}}$. In the following, we thus express the term in the exponent more generally as : $\frac{s}{\sqrt{G(s)}} = s^{\frac{\alpha}{2}}$.

Let us define the sine-Fourier transform of a function $f(x)$ in the $x-$ domain valid for $0 < x < \infty$ as

$$F(k) = \int_0^\infty f(x)\sin(kx)dx. \tag{E.10}$$

Taking the sine-Fourier transform of Eq. (E.9), we obtain

$$v(k,s) = \frac{v_0}{s}\frac{2k}{s^\alpha + k^2}. \tag{E.11}$$

This can be written as

$$v(k,s) = \frac{2kv_0}{k^2}\left(\frac{1}{s} - \frac{s^{\alpha-1}}{s^\alpha + k^2}\right). \tag{E.12}$$

Now, the Laplace inverse of

$$\left(\frac{s^{\alpha-1}}{s^\alpha + k^2}\right) \to E_{\alpha,1}\left[-k^2 t^\alpha\right], \tag{E.13}$$

where $E_{\alpha,\beta}$ is the generalized Mittag-Liffler function [78]

$$E_{\alpha,\beta}(z) = \sum_{n=0}^{\infty}\frac{z^n}{\Gamma(\alpha n + \beta)}. \tag{E.14}$$

Therefore, the inverse Laplace transform of Eq. (E.12) reads:

$$v(k,t) = \frac{2v_0}{k}\left(1 - E_\alpha\left[-k^2 t^\alpha\right]\right). \tag{E.15}$$

and inverting in k space, we obtain the transverse velocity field :

$$v(x,t) = 2v_0\int_0^\infty \frac{\sin(kx)}{k}\left(1 - E_\alpha\left[-k^2 t^\alpha\right]\right)dk. \tag{E.16}$$

This equation can be expressed more concisely by defining a new variable $\omega = kt^{\frac{\alpha}{2}}$. Then, the integral can be represented in terms of just one similarity variable:

$$v(x,t) = 2v_0\int_0^\infty \frac{\sin(\omega\eta)}{\omega}\left(1 - E_\alpha\left[-\omega^2\right]\right)d\omega, \tag{E.17}$$

where $\eta = \frac{x}{t^{\frac{\alpha}{2}}}$ is the similarity variable.

As a check for the convergence of the integral solution, consider the special case where $\alpha = 1$. This corresponds to the ordinary diffusion equation. Then, the integrals can be solved by noting that

$$E_{1,1}(-k^2 t) = \exp(-k^2 t). \tag{E.18}$$

Further,

$$\int_0^\infty \frac{\sin(kx)}{k} = \frac{\pi}{2}, \tag{E.19}$$

and

$$\int_0^\infty \frac{\sin(kx)}{k}\exp(-k^2 t) = \frac{\pi}{2}\operatorname{erf}\left(\frac{x}{2t^{\frac{1}{2}}}\right). \tag{E.20}$$

E.2 FRACTIONAL EQUATION

Although, we do not make extensive use of it, as an interesting mathematical aside, one way to model regimes of anomalous diffusion is to write down an analogue of Eq. (6.11), but with fractional derivatives (in time or space). A space fractional diffusion equation takes the form

$$\frac{\partial u}{\partial t} = D\frac{\partial^\alpha u}{\partial^\alpha x}, \tag{E.21}$$

where $\alpha = \frac{2}{\xi}$. Here, we have used fractional derivatives with respect to the spatial coordinates only and the fractional derivatives are interpreted in the sense described by Caputo [77]. Note, if $\alpha = 1$, we recover the one dimensional wave equation (half-wave equation), while for $\alpha = 2$ ($\xi = 1$), we obtain the ordinary diffusion equation. Similar to ordinary derivatives, a Fourier- transform of Eq. (E.21) can also be defined and leads to the general kernel

$$u(k,t) \sim \exp\left(t(-ik)^\alpha\right), \tag{E.22}$$

with a response time

$$t_r = \frac{1}{Dk^\alpha}. \tag{E.23}$$

Note, for $\alpha = 2$, we recover Eq. (6.13). Moreover, Eq. (E.23) corresponds dimensionally to a similarity solution of the form $\left(\frac{x}{t^{\frac{1}{\alpha}}}\right)$. For $\alpha = 4/3$, this gives us $\left(\frac{x}{t^{\frac{3}{4}}}\right)$ that is consistent with the super-diffusive growth of the width at early times in Fig. (6.2).

Note, from our observations in Fig. (6.2), we could also have started with a time fractional version of the diffusion equation in real space-time variables [77, 78] :

$$\frac{\partial^\alpha u}{\partial^\alpha t} = D\frac{\partial^2 u}{\partial x^2}. \tag{E.24}$$

Once again, we can take the Laplace transform in time domain and a sine-Fourier transform in x, to obtain Eq. (E.11) for the initial condition $v(0,s) = \frac{v_0}{s}$. Thus, the two approaches give the same solution. Note, the use of fractional derivatives naturally takes into account the non-locality implicit in the convolution in Eq. (E.2).

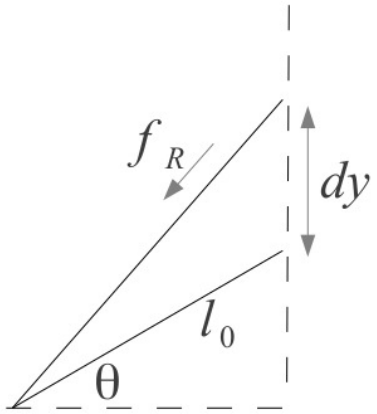

Figure E.1: A harmonic spring with equilibrium length l_0, initially lying at an angle θ in the $x-y$ plane. On e end of the spring is then moved to by an amount dy, to calculate the resultant force in the new position f_R.

E.3 NON-LINEARITY FROM HARMONIC SPRINGS

As a concluding remark, note that, although the spring networks we have considered are composed of harmonic springs, for high strains, the network response becomes non-linear. Although the actual mechanisms for the vanishing of the linear response in a disordered network of springs is fairly complex and involves a collective softness, the origins of nonlinearity can be traced to the simple picture depicted in Fig. (E.1). In particular, if we consider a spring with an equilibrium length l_0 lying at an angle θ in the $x-y$ plane, and move one of its ends by a small amount dy along the $y-$direction (for instance, the spring can be thought of the boundary spring that is sheared in the $y-$ direction), then the force along the direction of the spring is

$$f = -(\sqrt{(l_0 \sin\theta + dy)^2 + (l_o \cos\theta)^2} - l_0). \tag{E.25}$$

By squaring and Taylor expanding the terms inside the square root, we find the force

$$f \approx -\left(dy \sin\theta + \frac{(dy)^2}{2l_0}\right). \tag{E.26}$$

Consequently, the return force in the direction of shearing is

$$f_y \approx -\left(dy \sin\theta + \frac{(dy)^2}{2l_0}\right)\frac{(dy + l_0 \sin\theta)}{l_0}, \tag{E.27}$$

that yields

$$f_y \approx -\frac{1}{l_0}\left(dy\, l_0 \sin^2\theta + \frac{3}{2}(dy)^2 \sin\theta + \frac{dy^3}{2l_0}\right). \tag{E.28}$$

Thus, the dominant non-linearity (second term on the right) is quadratic in displacement dy. For a more rigorous argument that also correctly accounts for the vanishing linear response, see [2].

F

IDEAS FOR FURTHER WORK ON THERMAL AND QUANTUM FLUCTUATIONS

As discussed in Chapter 6, a two dimensional random network of springs becomes rigid when the mean connectivity $\langle z \rangle$ exceeds a critical isostatic value $z_c = 4$. Here, the onset of rigidity is a purely geometrical or mechanical phenomenon. In Chapter 5, we discussed that thermal fluctuations can introduce rigidity in a chain of (un-stressed) non-linear springs, that a-priori has no linear response. Similarly, a network of freely jointed chains that are often used as a simple model for polymers, can display a purely entropic elasticity with a shear modulus that grows linearly with temperature, i.e., $G \sim T$ [54].

Many systems however fall in an intermediate regime, where the rigidity arises from an interplay between network geometry and coupling to a source of fluctuation. In a recent study on such a model (a two dimensional random network of diluted springs), it is shown that the shear modulus scales sub-linearly with temperature, i.e., $G \sim T^{\alpha}$, with $0 < \alpha < 1$ [54]. Note, $\alpha = 1$ corresponds to the regime of purely entropic elasticity (such as freely jointed chains), while $\alpha = 0$ gives a shear modulus that is independent of temperature as for instance, can be expected for elastic spring networks well above the isostatic point, i.e., $z \gg z_c$.

However, so far much less is known about the role of quantum fluctuations (zero point motion) on the mechanical properties of fragile systems. For example, at the microscopic level, network glasses can be viewed as a random network of harmonic springs. An intriguing question then is: can the quantum zero point motion of network nodes induce the equivalent of an entropic (thermally induced) rigidity as the temperature is lowered ?

Thus, if amorphous materials can indeed be modelled as a random network of harmonic springs with a tune-able connectivity, then close the isostatic point, their elastic properties and specific heat can be expected to be profoundly effected by network connectivity and quantum and thermal fluctuations [80]. In this final chapter, we therefore discuss some initial ideas exploring this direction, by studying the effects of thermal and

quantum fluctuations on the rigidity of a random network of harmonic springs that are derived from jammed packings prepared at vanishingly small pressure. We discuss a simple method that allows us to approximately model both thermal and quantum fluctuations within a classical simulation, by coupling the system to a source of noise given by the Bose-Einstein spectrum. In the low temperature limit, this allows us to study the effects of quantum zero point motion within a purely classical approximation, while the high temperature limit, allows us to study the role of purely thermal fluctuations.

F.1 APPROXIMATE METHOD TO SIMULATE QUANTUM ZERO POINT ENERGY

Due to quantum fluctuations, the energy of the system at zero temperature, called the zero point energy, is larger than the potential energy minimum. This property is a direct consequence of the quantization of the energy of the vibrational modes. An intriguing, albeit approximate method, that allows us to incorporate zero point motion within a classical description of particle dynamics, is to consider a Langevin equation of the form Eq. (5.1), but with the source of Gaussian noise replaced with coloured noise with an appropriate power spectral density. This method thus consists of modelling the zero point motion as a quantum bath, that is analogous to a thermal bath, but with a different source of noise. In this way, the correct zero point energy for a harmonic oscillator can be obtained [68, 75, 73].

What is the nature of the noise term ? In the next sub-section, we outline an intuitive method to see the appropriate power spectral density of the noise term that allows us to correctly obtain the energy of a simple harmonic oscillator. We then apply this method to study a one dimensional chain of harmonic oscillators and then, a two dimensional random network of harmonic springs.

F.1.1 *Simple harmonic oscillator*

Consider the equations of motion for a simple harmonic oscillator, akin to the Langevin equation that we considered in Chapter 5 Eq. (5.1), leaving the noise source $\Theta(t)$ as yet unspecified:

$$\frac{dx}{dt} = v, \tag{F.1}$$

$$\frac{dv}{dt} = -\omega_0^2 x - \gamma v + \sqrt{2\gamma}\theta(t) \tag{F.2}$$

where, x is the displacement from the equilibrium position, v is the speed, γ is the external drag and $\Theta(t)$ is a source of fluctuation. Here, we have set mass $m = 1$ and the oscillator frequency is ω_0. Fourier transforming the equations Eq. (F.1) using $X(\omega) = \int x(t)e^{-i\omega t}$,$V(\omega) = \int v(t)e^{-i\omega t}$ we obtain

$$X(\omega) = \sqrt{2\gamma}\frac{\Theta(\omega)}{\omega_0^2 - \omega^2 + i\omega\gamma}, \tag{F.3}$$

$$V(\omega) = \sqrt{2\gamma}\frac{i\omega\Theta(\omega)}{\omega_0^2 - \omega^2 + i\omega\gamma}. \tag{F.4}$$

The power spectral density corresponding to the random variables $x(t), v(t)$ is $|X(\omega)|^2, |V(\omega)|^2$ respectively. Therefore, the ensemble averaged energy of the oscillator is

$$E(\omega) = \int \frac{d\omega}{2\pi}\left(\frac{1}{2}\omega_0^2|X(\omega)|^2 + \frac{1}{2}|V(\omega)|^2\right), \tag{F.5}$$

$$= \int \frac{d\omega}{2\pi}\gamma\frac{\omega^2 + \omega_0^2}{\left(\omega^2 - \omega_0^2\right)^2 + \omega^2\gamma^2}\Theta(\omega). \tag{F.6}$$

Here, $\Theta(\omega)$ is the power spectral density of the noise.

For small damping γ, the poles of Eq. (F.6) are $\omega = \pm\omega_0 \pm i\gamma/2$, to leading order in γ. Solving by residues, we find that for a constant $\Theta(\omega)$, integration of Eq. (F.6) gives a constant that is independent of the drag γ. If we choose the constant $\Theta(\omega) = k_B T$ (independent of ω as in the Langevin equation), integration of Eq. (F.6) , reproduces the classical equipartition theorem, where the energy is just equal to the the thermal energy.

Similarly, for a frequency dependent $\Theta(\omega)$, integration of Eq. (F.6) gives $E \approx \Theta(\omega_0)$, to leading order in γ. Hence, by choosing

$$\Theta(\omega) = \hbar|\omega|\left(\frac{1}{2} + \frac{1}{\exp\left(\frac{\hbar\omega}{k_B T}\right) - 1}\right) \tag{F.7}$$

and a value for γ small enough compared to the characteristic frequency ω_0, we can ensure that the energy of the oscillator is given by the Bose-Einstein distribution Eq. (F.7) including the zero point energy.

Note, in these equation, no operators are involved. This is truly a classical approximation of the quantum zero point energy, where we are assuming that the quantum fluctuations are akin to thermal fluctuations, causing the particle position and velocity to fluctuate in time. For a detailed derivation of this classical approximation beginning with the coherent state description, see ref [68].

F.2 CHAIN OF HARMONIC OSCILLATORS

As a first step towards checking whether the above equations correctly reproduce the energy of a harmonic oscillator, we simulate a one dimensional chain of $N = 1024$ harmonic oscillators, where each particle is coupled to a source of noise $\Theta(t)$ and drag γ, and therefore satisfies an equation of the form Eq. (F.1). For more details on how to construct an approximate noise source in time domain that has the power spectral density given in Eq. (F.7), see section F.4.

In Fig. (F.1), we plot the numerically obtained energy (red circles) of the chain of harmonic oscillators against the Temperature, and compare it with the analytic expression given by the Bose-Einstein distribution Eq. (F.7), finding a reasonably good agreement. In these plots, we have used reduced units where energy is specified in units of ka^2, where k is the bare spring constant and a is the lattice spacing. In Fig. (F.2), we also verify that in equilibrium, the energy is equally partitioned between the quadratic degrees of freedom (i.e., the kinetic and potential energies). Here, the equilibration time is set by the inverse of the drag coefficient γ.

F.3 RANDOM NETWORK OF HARMONIC SPRINGS

We now study a random network of harmonic springs derived from jammed packings (see Fig. 6.1) that have been prepared at a vanishingly small pressure so that the mean overlap between disks δ is nearly 0. For such networks of harmonic springs, the shear modulus scales linearly with the excess coordination number $G \sim dz = z - z_c$, where z is the average coordination number per node and $z_c = 4$ is the critical coordination num-

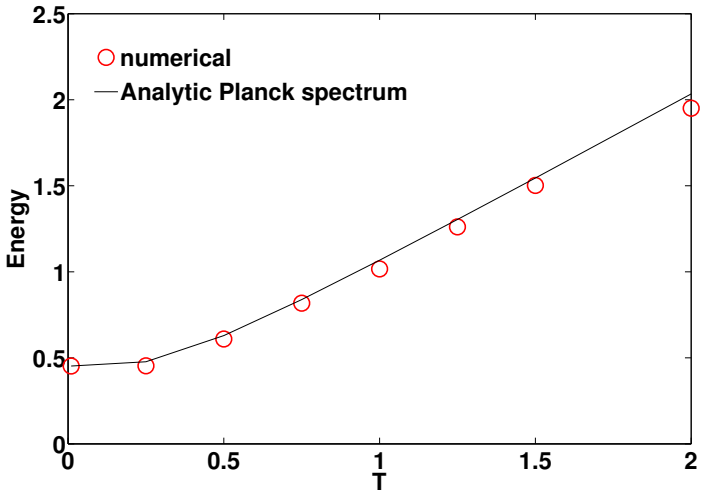

Figure F.1: Comparison of analytical Planck spectrum (solid black curve) against the energy of a chain of harmonic oscillators obained numerically (red dots). Here, $\hbar\omega_0 = 1.0$. Note, unlike the case of a classical simulation where the energy at zero temperature would be zero, here the energy levels off to around 0.45, close to the expected zero point energy. Here, energy is measured in units of ka^2, where k is the bare spring constant and a is the equilibrium lattice spacing.

ber in two dimensions. At the same time, the bulk modulus remains finite at the critical point and is nearly independent of dz as we move further away from the critical point.

We now couple the nodes of the two dimensional network of harmonic springs to a source of noise, modelled by the Bose-Einstein spectrum, Eq. (F.7) and study the equilibrium properties of the network. As a first step, in Fig. (F.3), we plot the numerically obtained energy (red circles) of this system against the Bose-Einstein distribution Eq. (F.7), where we find a reasonably good match for a range of ratios $\hbar\omega_0/k_B T$.

F.3.1 *Fluctuation induced rigidity*

Next, we study the long wavelength small frequency longitudinal and shear modes, using a procedure similar to the one

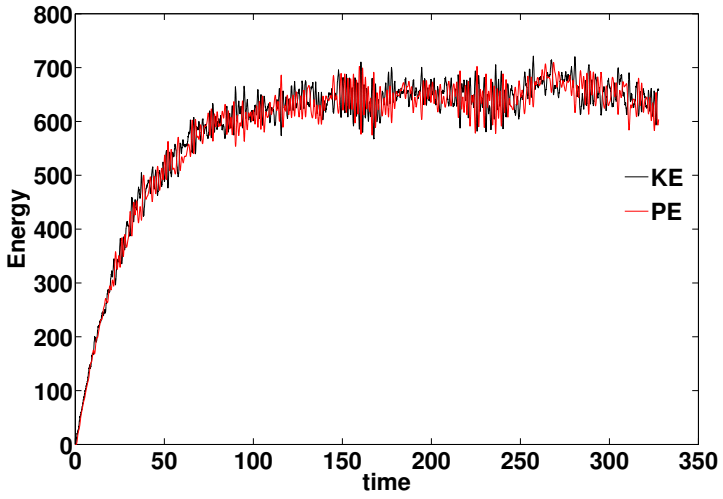

Figure F.2: Confirmation of the equipartition between kinetic (black) and potential (red) energies in a chain of harmonic oscillators at $\hbar = 1.0$ and $T = 1.25$.

outlined in Chapter 4. Note, the Bose-Einstein distribution has the following asymptotic forms:

$$\Theta(\omega) = \frac{1}{2}\hbar|\omega|; T \to 0 \tag{F.8}$$

$$\Theta(\omega) = k_B T; T \to \infty, \tag{F.9}$$

$$\tag{F.10}$$

that correspond to the quantum and classical limits respectively. In Fig. (F.4), we therefore probe these limits and plot the numerically obtained dispersion curves (obtained analogously to the procedure described in Chapter 5) for the shear modes, as a function of reduced temperature T (left panel) and reduced $\hbar$ (right panel). As expected from the physics near the vicinity of the critical point, the slopes of the dispersion curves explicitly depend upon the energy of the fluctuation, i.e., the temperature or $\hbar$. Moreover, for random networks derived from jammed packings, the bulk modulus remains finite at the critical point and accordingly, the longitudinal dispersion curves remain nearly independent of temperature (see scaling in Figs. (F.6)-(F.7)).

In order to check the correctness of this procedure ,i.e., the use of hydrodynamical modes to estimate the elastic modulus of spring networks, we plot in Fig. (F.5), the scaling of the shear (black circles) and bulk modulus (blue circles) as a function of the energy of pre-compression for spring networks derived

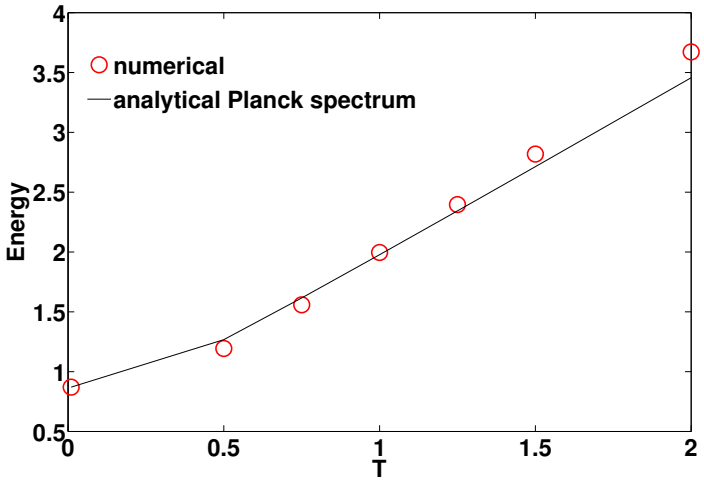

Figure F.3: Comparison of analytical Planck spectrum (solid black curve) against the energy for a random network of springs obained numerically (red dots). Here, $\hbar\omega_0 = 1.0$. Note, unlike the case of a classical simulation where the energy at zero temperature would be zero, here the energy levels off to around 0.9, close to the expected zero point energy that is 1.0 in two dimensions. Here, energy is measured in units of ka^2, where k is the bare spring constant and a is the average equilibrium lattice spacing.

from jammed packings with varying initial compression and with vanishingly small temperature, so as to probe the elasticity of the network that stems only from the geometry of the network. In particular, for an interaction potential of the form δ^α, where δ is the average initial overlap between disks, the shear modulus is expected to scales as $G \sim \delta^{\alpha-3/2}$ and the bulk modulus as $B \sim \delta^{\alpha-2}$. For harmonic interaction with $\alpha = 2$, this leads to $G \sim \delta^{1/2}$ and $B \sim \delta^0$. In this case, the energy of the packing due to pre-compression is $E \sim \delta^2$ (harmonic potential), and therefore, $G \sim E^{1/4}$ with an exponent 0.25. In Fig. (F.5), we find a scaling with an exponent approximately 0.23, close to the expected value, while the bulk modulus remains independent of the energy.

In Figs. (F.6-F.7), we show the analogous scaling we obtain when we couple the spring network that is close to the critical point, to a source of finite temperature and $\hbar$. In this case, we find that the scaling differs from that expected at a finite pre-compression. Rather, the shear modulus seems to scale as $G \sim (k_B T)^{0.4}$ and $G \sim (\hbar\omega_0)^{0.4}$, in units of the square of the inverse

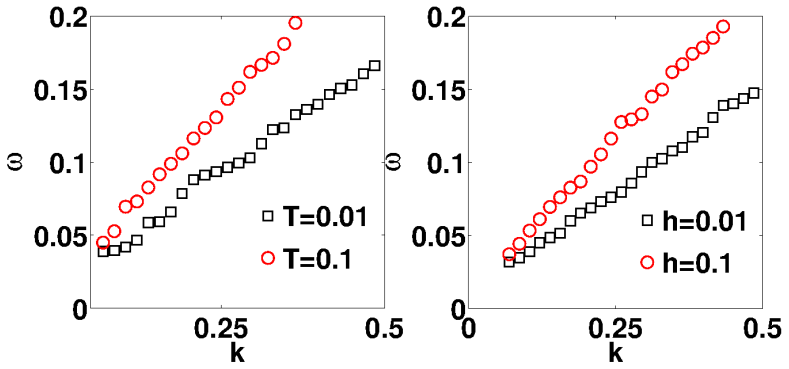

Figure F.4: The onset of shear rigidity due to thermal fluctuations (left panel) and classical approximation to quantum fluctuations (right panel). We define the shear rigidity as the square of the slopes of these curves.

lattice spacing. In these plots, the value of T and $\hbar$ are chosen so that the energy induced by fluctuations is roughly comparable to the energies of the pre-compressed packings in Fig. (F.5) to allow for a more meaningful comparison.

F.4 SIMULATION

F.4.1 *Planck Spectrum*

The numerical implementation of the quantum bath reduces to generating a colored noise with a power spectral density $\Theta(\omega)$. Here, we adopt the numerical scheme suggested in reference [73, 74, 75].

For a continuous noise, we introduce the filter

$$H(\omega) = \sqrt{\Theta(\omega)}. \tag{F.11}$$

and denote $H(t)$ as the inverse Fourier transform of $H(\omega)$. The noise $\Theta(t)$ can then be obtained by convolving $H(t)$ with a source of random noise $r(t)$, that has a power spectral density $R(\omega) = 1$. Therefore,

$$\Theta(t) = \int_{-\infty}^{\infty} H(s)r(t-s)ds. \tag{F.12}$$

The power spectral density of the resulting noise is $|H(\omega)|^2 R(\omega) = \Theta(\omega)$, which is the desired power spectral density.

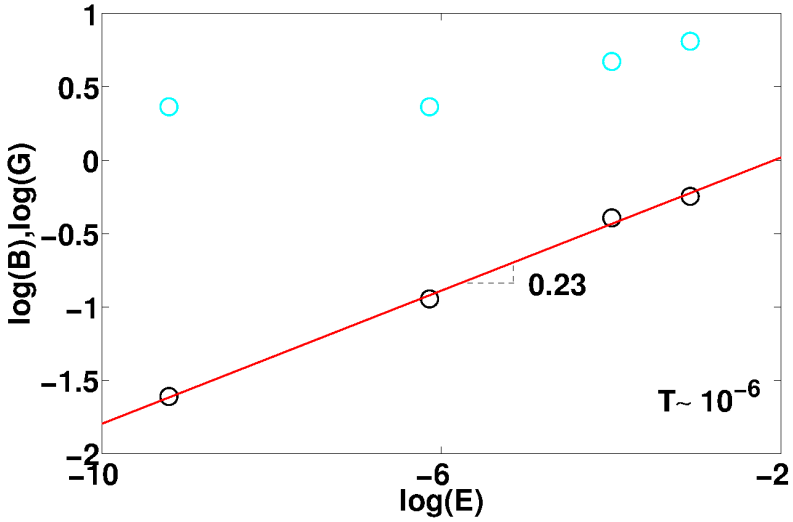

Figure F.5: The numerically computed shear (black circles) and bulk modulus (blue circles) plotted against the energy of the spring networks derived from jammed packings at various pre-compressions. These plots are obtained at a vanishingly small temperrature , so the the moduli scale with the pre-compression or network geometry. We find the bulk modulus is nearly independent of the pre-compression while the shear modulus scales approximately as $G \sim E^{1/4} \sim \delta^{1/2}$.

Numerically, this can be implemented as follows. The filter $H(\omega)$ is first discretized in $2N$ values with steps $d\omega$ over an interval $[-\Omega_{max}, \Omega_{max}]$:

$$H_k = H(kd\omega), k = -N \cdots N-1. \tag{F.13}$$

On physical grounds, the cut-off frequency can be chosen to be around the maximum frequency for a harmonic oscillator $\sqrt{K/m}$, where K is the spring constant and m is the mass. Subsequently, we take the discrete Fourier transform of H_k:

$$H_n = \frac{1}{2N} \sum_{-N}^{N-1} H_k \cos\left(\frac{\pi}{N} kn\right). \tag{F.14}$$

Finally, we perform the discrete convolution

$$\Theta_n = \sum_{-N}^{N-1} H_m r_{n-m}, \tag{F.15}$$

where r is a normal random variable.

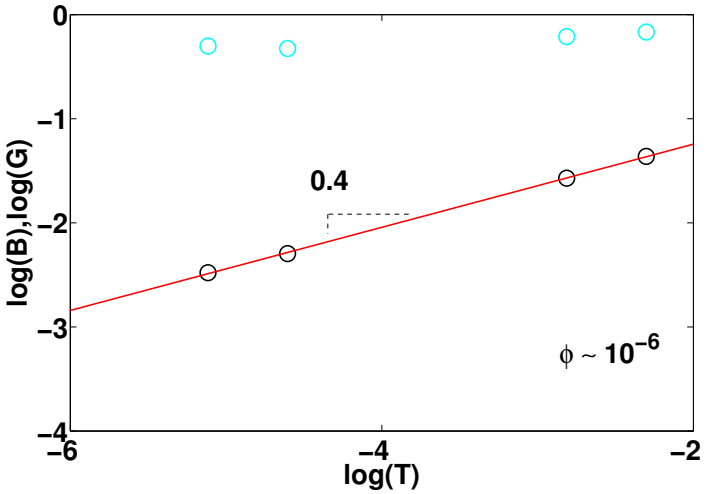

Figure F.6: The numerically computed shear (black circles) and bulk modulus (blue circles) plotted against the thermal energy for nearly isostatic spring networks derived from jammed packing at vanishingly small pre-compression ϕ.

F.4.2 *Limiting forms*

Note, the classical high temperature limit of the Planck spectrum is $k_B T$. Thus, the same procedure outlined above can be used to simulate a classical system coupled to a heat bath, as in Chapter 5. Further, for the numerical integration, we use a modified form of the velocity Verlet method that in the limit $\hbar \to 0, k_B T \to 0$ and drag $\gamma \to 0$, reduces to the velocity verlet method [71].

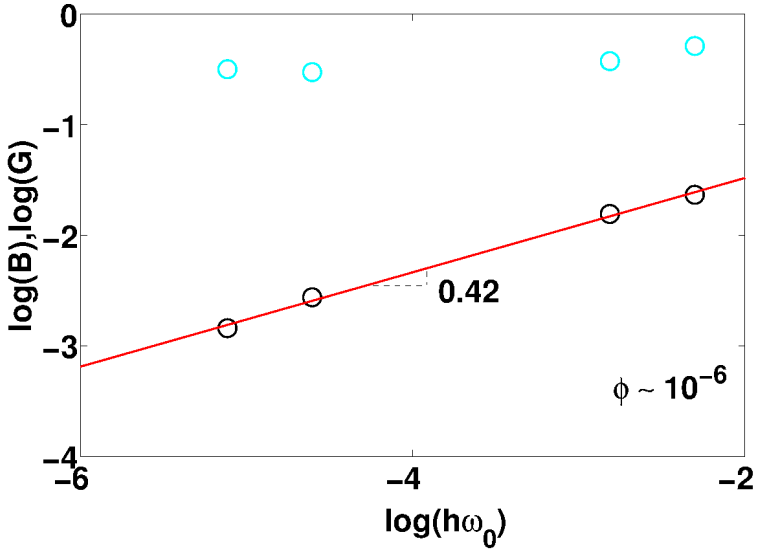

Figure F.7: The numerically computed shear (black circles) and bulk modulus (blue circles) plotted against the quantum energy for nearly isostatic spring networks derived from jammed packing at vanishingly small pre-compression ϕ.

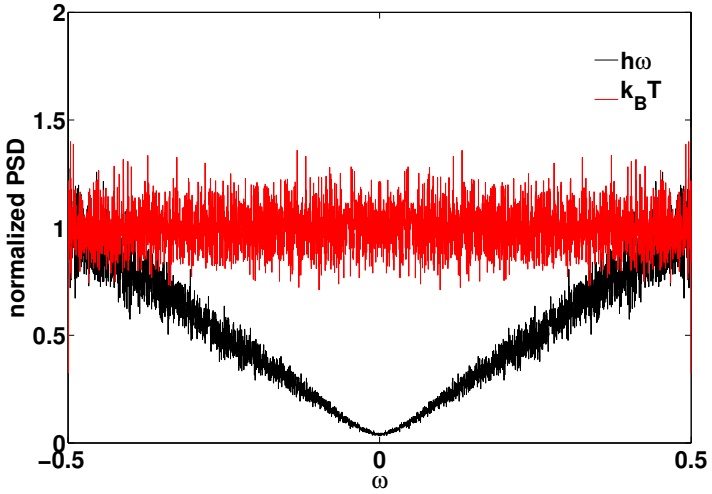

Figure F.8: Plots of the Planck spectrum obtained numerically for its asymptotic forms of high frequency (black) and high temperatures (red). The high frequency power increases linearly with frequency and corresponds to the quantum zero point motion, while the power spectrum density is a constant independent of frequency and proportional to $k_B T$ in the high temperature (classical) limit.

BIBLIOGRAPHY

[1] V. Vitelli and M. van Hecke, Euro Physics News **43** , 6 (2012).

[2] M. Wyart, H. Liang, A. Kabla and L. Mahadevan, Phys. Rev. Lett. **101**, 21 (2008).

[3] W.G. Ellenbroek, Z. Zeravcic, W.V. Sarloos and M.V. Hecke, Eur. Phys. Lett. **109**, 34004 (2009).

[4] B. Tighe, Phys. Rev. Lett. **107**, 15 (2011).

[5] L. D. Landau and E.M. Lifshitz, *Theory of elasticity* (Pergamon press, 1970).

[6] V. F. Nesterenko, *Dynamics of Heterogeneous Materials* (Springer-Verlag, New York, 2001), Chap. 1.

[7] S.V.D Wildenberg, R.V. Loo and M.V. Hecke, arXiv:1304.6392 [cond-mat.soft] (2013).

[8] S. R. Waitukaitis, L. K. Roth, V. Vitelli and H. M. Jaeger, Eur. Phys. Lett. **102** 2013.

[9] S.Ulrich, N. Upadhyaya, B.V. Opheusden and V. Vitelli, arXiv:1307.7665 (2013).

[10] A. J. Heeger, S. Kivelson, J. R. Schrieffer and W.-P. Su, Rev. Mod. Phys. **68**, 13 (1996).

[11] S. Sen, J. Hong, J. Bang, E. Avalos, and R. Doney, PhysicsReports **462**, 21-66 (2008).

[12] A. Spadoni and C. Daraio, Proceedings of the National Academy of Sciences **107**, 7230 (2010).

[13] N. Boechler, G. Theocharis, and C. Daraio, Nat. Mat. **10**, 665 (2011).

[14] V. F. Nesterenko, A. N. Lazaridi, and E. B. Sibiryakov, Prikl. Mekh. Tekh. Fiz. **36**, 19 (1995)[J. Appl. Mech.Tech. Phys., **36**, 166 (1995)].

[15] V. F. Nesterenko, J. Phys. IV, **4**, C8-729 (1994).

[16] V. F. Nesterenko, C. Daraio, E. Herbold, S. Jin, Phys. Rev. Lett., **95**, 158702 (2005).

[17] S. Job, F. Melo, A. Sokolow, and S. Sen, Granular Matter **10**, 13 (2007).

[18] A. N. Lazaridi and V. F. Nesterenko, Prikl. Mekh. Tekh. Fiz., textbf26, 115 (1985)[J. Appl. Mech. Tech. Phys., **26**, 405 1985)].

[19] A. Sokolow, E.G. Bittle, S. Sen, Europhys. Lett., **77**, 24002 (2007).

[20] E. Somfai, J. N. Roux, J. H. Snoeijer, M. van Hecke, and W. van Saarloos, Phys. Rev. E **72**, 021301 (2005).

[21] C. Daraio, V.F. Nesterenko, S. Jin Strongly nonlinear waves in 3d phononic crystals. In: Furnish, M.D., Gupta, Y.M., Forbes, J.W. (eds.) Shock compression of condensend matter 2003, Proceedings of the conference of the American physical society topical group on shock compression of condensed matter, vol 706, pp. 197200, AIP (2004).

[22] E. J. Hinch and S. Saint-Jean, Proc. R. Soc. A, **455**, 3201 (1999).

[23] C. Coste, E. Falcon, and S. Fauve, Phys. Rev.E **56**, 6104 (1997).

[24] C. Daraio, V. F. Nesterenko, E. B. Herbold, and S. Jin, Phys. Rev. E **72**, 016603 (2005).

[25] S. Sen, J. Hong, J. Bang, E. Avalos, and R. Doney, Physics Reports **462**, 21 (2008).

[26] L. R. Gómez, A. M. Turner, M. van Hecke, and V. Vitelli, Phys. Rev. Lett. **108**, 058001 (2012).

[27] L. R. Gómez, A. M. Turner and V. Vitelli, Phys. Rev. E **86**, 041302 (2012).

[28] L. Vergara, Phys. Rev. Lett. **95**, 108002 (2005).

[29] F. S. Manciu and S. Sen, Phys. Rev. E **66**, 016616 (2002).

[30] M. P. Allen and D.J. Tildsey, Computer simulation of liquids (Oxford, New York, 1987).

[31] C. Daraio, D. Ng, V. F. Nesterenko, F. Fraternali, Phys. Rev. E. **82**, 036603 (2010).

[32] V. F. Nesterenko, J. Appl. Mech. Tech. Phys. **5**, 733 (1984).

[33] S. Sen, J. Hong, J. Bang, E. Avalos, and R. Doney, Physics Reports **462**, 21 (2008).

[34] M. Manjunath, A.P. Awasthi, and P.H. Geubelle, Phys. Rev. E **85**, 031308 (2012).

[35] S. van den Wildenberg, R. van Loo and M. van Hecke, arXiv:1304.6392, (2013).

[36] K. Ahnert and A. Pikovsky, Phys. Rev. E **79**, 026209 (2009).

[37] E. Aŕalos, D. Sun, R.L. Doney and S. Sen, Phys. Rev. E **84**, 046610 (2011).

[38] O.V. Zhirov, A.S. Pikovsky and D.L. Shepelyansky, Phys. Rev. E **83**, 016202 (2011).

[39] A. Tichler *et al*, Phys. Rev. Lett., **111**, 048001 (2013).

[40] R. Zwanzig and M. Bixon, Phys. Rev. A **2**, 2005 (1970).

[41] M.H. Ernst, E.H. Hauge and J.M.J. Leeuwen, Phys. Rev. A **4**, 2055 (1971).

[42] M.H. Ernst, Physica D **47**, 198 (1991).

[43] B.E. McDonald and D. Calvo , Phys. Rev. E, **85**, 066602 (2012).

[44] M. Wadati, J. Phys. Soc. Jap. **59**, 12 (1990).

[45] N. Upadhyaya, L. R. Gomez and V. Vitelli, arXiv:1304.6692 , (2013).

[46] V. Yakhot and Z. She, Phys. Rev. Lett., **60**, 18 (1988).

[47] O. Narayan and S. Ramaswamy, Phys. Rev. Lett., **89**, 048001 (2002).

[48] M. Kardar, *Statistical Physics of Fields*, (Cambridge University Press, 2007).

[49] P. Rosenau, Phys. Lett. A **118**, 5 (1986).

[50] A. Yethiraj, Royal Soceity of Chemistry. **3**, 1099-1115 (2007).

[51] D.E. Chang, J.I. Cirac and H.J. Kimble, Phys. Rev. Lett. **110**, 113606 (2013).

[52] Z. Cheng, J. Shu, W.B. Russel and P.M. Chaikin, Phys. Rev. Lett. **85**, 7 (2000).

[53] M. Sheinman, C.P. Broedersz and F.C. MacKintosh, Phys. Rev. Lett. **109**, 238101 (2012).

[54] M. Dennison, M. Sheinman, C. Storm and F.C. MacKintosh, arXiv:1304.3500 (2013) .

[55] A.S. Davydov, J. Theor. Bio., **66**, 379 (1977).

[56] T. Dauxois and M. Peyrard, *Physics of solitons* (Cambridge University Press, 2006).

[57] C. S. O'Hern, L. E. Silbert, A. J. Liu, and S. R. Nagel, Phys. Rev. E. **68** 011306 (2003).

[58] I. Atsushi, L. Berthier and G. Biroli, J. Chem. Phys. **138** 12A507 (2013)

[59] N. Xu, T. K. Haxton, A. J. Liu, and S. R. Nagel, Phys. Rev. Lett. **103** 245701 (2009).

[60] We are using "soliton" and "solitary wave" interchangeably to refer to a localized lump of of energy; we do not assume anything about the equations being integrable.

[61] For many waves or solitons, differentiating E with respect to P would give the group velocity or the speed of the wave's propagation, but this does not work for this case. (P is not the canonical momentum.)

[62] N. Upadhyaya, A. M. Turner and V. Vitelli, arXiv:1304.6684 , (2013).

[63] N.G. Van Kampen, *Stochastic processes in physics and chemistry* (Elsevier science publishers, 2007).

[64] E. Arevalo, F.G. Mertens, Y. Gaididei and A.R. Bishop, Phys. Rev. E. **67**, 016610 (2003).

[65] D.T. Gillespie, *Markov processes: an introduction for physical scientists* (Academic press, 1992).

[66] D.S. Lemons, *An introduction to stochastic processes in physics* (The John Hopkins university press, 2002).

[67] C.W. Gardiner, *Handbook of Stochastic Methods* (Springer, 1997).

[68] C.W. Gardiner and P. Zoller, *Quantum noise* (Springer, 2000).

[69] J.P. Boon and S. Yip, *Molecular Hydrodynamics* (McGraw Hill Inc, 1980).

[70] J.P. Hansen and I.R. McDonald, *Theory of simple liquids* (Elsevier, 2006).

[71] M.P. Allen and D.J. Tildsey, *Computer simulation of liquids* (Oxford, New York, 1987).

[72] N. Upadhyaya, *Brownian dynamic simulation of dusty plasma*, Master thesis 2010, http://hdl.handle.net/10012/5070.

[73] J.L. Barrat and D. Rodney, J. Stat. Phys., **144**, 677-689 (2011).

[74] I am grateful to Prof. Barrat for sharing a version of their simulation code to explain some details regarding their paper.

[75] H. Dammak *et. al.* , Phys. Rev. Lett. **103**, 190601(2009).

[76] M. Saadatfar and Muhammad Sahimi, Phys. Rev. E. **65**, 036116, (2002).

[77] I. Podlubny, *Fractional differential equations* (Academic Press, 1999).

[78] Y. Povstenko, Fractional calculus and applied analysis, **11**, 3, (2008).

[79] H.V. Beijeren, arXiv:1106.3298 (2012).

[80] M.F. Thorpe, Journal of Non-Crystalline Solids, **57** (1983) 355-370.